Biomaterials 32 (2011) 7609–7615

Contents lists available at ScienceDirect

Biomaterials

journal homepage: www.elsevier.com/locate/biomaterials

The induction of epigenetic regulation of PROS1 gene in lung fibroblasts by gold nanoparticles and implications for potential lung injury

Cheng-Teng Ng [a,b], S. Thameem Dheen [a], Wai-Cheong G. Yip [a], Choon-Nam Ong [c], Boon-Huat Bay [a,*], Lin-Yue Lanry Yung [b,*]

[a] Department of Anatomy, Yong Loo Lin School of Medicine, National University of Singapore, Singapore 117597, Singapore
[b] Department of Chemical & Biomolecular Engineering, Faculty of Engineering, National University of Singapore, Singapore 117576, Singapore
[c] Department of Epidemiology and Public Health, National University of Singapore, Singapore 117597, Singapore

ARTICLE INFO

Article history:
Received 27 May 2011
Accepted 17 June 2011
Available online 20 July 2011

Keywords:
Gold nanoparticles
miR-155
PROS1
Methylation
Nanotoxicity
Epigenetic

ABSTRACT

Advances in nanotechnology have given rise to the rapid development of novel applications in biomedicine. However, our understanding in the risks and health safety of nanomaterials is still not complete and various investigations are ongoing. Here, we show that gold nanoparticles (AuNPs) significantly altered the expression of 19 genes in human fetal lung fibroblasts (using the Affymetrix Human Gene 1.0 ST Array). Among the differentially expressed genes, up-regulation of microRNA-155 (miR-155) was observed concomitant with down-regulation of the PROS1 gene. Silencing of miR-155 established PROS1 as its possible target gene. DNA methylation profiling analysis of the PROS1 gene revealed no changes in the methylation status of this gene in AuNP-treated fibroblasts. At the ultrastructural level, chromatin condensation and reorganization was observed in the nucleus of fibroblasts exposed to AuNPs. The findings provide further insights into the molecular mechanisms underlying toxicity of AuNPs and their impact on epigenetic processes.

1. Introduction

Engineered nanomaterials are a class of materials that possess at least one dimension in the range of 1–100 nm [1]. Due to their unique physical and chemical properties, nanomaterials have been widely explored in biomedical and healthcare application such as medical imaging and diagnosis, pharmaceuticals, drug therapeutics, and various other products [2]. Although the use of nanomaterials for healthcare purposes has unique advantages, the potential health hazardous effects are currently insufficiently addressed. Their potentially wide biomedical applications reflect an increasing need to ascertain their health impact before application. For example, gold nanoparticles (AuNPs) are widely utilized in bioimaging and in biosensing due to their unique plasmonic properties [3,4]. At the same time, the toxicity of AuNPs has been reported [5,6] and is dependent on their shape, size and duration of exposure [3].

miRNAs contain approximately 22 nucleotides and are cleaved by a nuclease (Dosha) before transported out from nucleus to the cytoplasm where post-transcription editing by an endoribonuclease (Dicer) takes place [7]. The resulting miRNAs, together with cellular complex, forms a miRNA-complex (known as microribonucleoproteins (miRNPs) or miRNA-induced silencing complexes) which inhibits the protein translation. The most conclusive evidence that miRNA regulates protein synthesis are derived from studies showing that their seed region binds to the 3′ untranslated region of protein-coding mRNAs and thus represses protein translation [8–10]. miRNAs are reported to control a wide repertoire of cellular processes which include apoptosis, metabolism, development, erythropoiesis, differentiation and oocytes maturation [11–14]. Although present data are based on the considerable amount of effort in research study, exact roles of miRNAs still remain obscure. Aberrant expression of miRNAs has been reported to be implicated in pathogenesis [15–19] and not surprising, in carcinogenesis [20–22]. It may also be noted that certain miRNAs expression in several types of cancer is apparent [20,23,24]. We have recently reported that AuNPs decreased cell proliferation and induced autophagy associated with oxidative stress in human lung fibroblast *in vitro* [25,26].

In this study, we evaluated the effects of AuNPs on the genome as well as studied the epigenetic changes of human lung fibroblasts following cellular uptake of the NPs.

* Corresponding authors. Tel.: +65 6516 1699.
E-mail addresses: boon_huat_bay@nuhs.edu.sg (B.-H. Bay), cheyly@nus.edu.sg (L.-Y. Lanry Yung).

0142-9612/$ – see front matter © 2011 Elsevier Ltd. All rights reserved.
doi:10.1016/j.biomaterials.2011.06.038

2. Materials and methods

2.1. Cell culture

MRC5 human fetal fibroblasts purchased from American Type Culture Collection (ATCC) were cultured in Rosewell Park Memorial Institute (RPMI 1640) medium (Invitrogen) supplemented with 10% heat-inactivated Fetal Bovine Serum (FBS) (Hyclone) and antibiotics (100 units/ml penicillin and 100 μg/ml streptomycin from Invitrogen). Primary small airway epithelial cells (SAEC) purchased from Lonza (Basel, Switzerland) were cultured as described earlier by Carayol et al. [27,28] in Small Airway cells Growth Medium (SAGM) from Bio-Whittaker (Walkersville). Cells were maintained at humidified atmosphere of 37 °C in a 5% CO_2 incubator.

2.2. AuNP preparation and treatment

AuNP, 20 nm in diameter, were synthesized by citrate reduction of gold salts following the methodology as previously described [26]. The AuNP colloidal solution was then sterile filtered before using.

The monolayer cultured cells were treated with or without AuNPs at a final concentration of 1 nM (derived from previous studies [25,26] for 48 h or 72 h).

2.3. Transmission electron microscopy (TEM)

Cells were fixed in 2.5% glutaraldehyde for 1 h followed by post-fixation with 1% osmium tetroxide and potassium ferrocyanide (Agar Scientific) for 1 h at room temperature. The samples were then dehydrated in an ascending series of ethanol and embedded in araldite (Ted Pella). Ultrathin sections were cut and mounted on formvar-coated copper grids. Sections were doubly stained with uranyl acetate (BDH) and lead citrate (BDH) and viewed under a Philips EM280S transmission electron microscope. Elemental analysis was performed using the Philips EDAX Microanalysis coupled with a CM120 BioTWIN electron microscope.

2.4. Human global Gene Array

Affymetrix Human Gene 1.0 ST Array experimentation (comprising labeling, hybridization, scanning and data analysis) was conducted by Origen Laboratories Pte Ltd (Singapore). Total RNA of each sample was extracted using RNeasy Mini Kit (Qiagen) following the manufacturer's user guide. Briefly, the cells were first lysed before equal volume of 70% ethanol was added. The homogenized lysate was transferred to the RNeasy MinElute Spin Column and centrifuged for 15 s at 13200 rpm. Several washes were performed to eliminate carry-over contaminants before RNA elution using RNase-free water.

2.5. cDNA synthesis/TaqMan® MicroRNA RT-PCR and quantitative real time PCR

Total RNA was isolated from MRC5 cells using RNeasy Mini Kit and mirVana™ miRNA Isolation Kit (Ambion) according to the manufacturers' instructions. TaqMan® MicroRNA RT-PCR was performed to validate that the expression of the mature miRNA 155 (capitalized 'miR'-155) was correlated to what we observed from microarray data.

1 μg of RNA was reverse transcribed using commercially purchased Super ScriptTM III First-Strand Synthesis System for RT-PCR kit (Invitrogen). RNA is first incubated with a random hexamer at 65 °C and then quickly chilled on ice. Other components such as dNTPs, RNase inhibitor, reverse transcriptase and RT buffer were added before incubated for 10 m, 25 °C followed by 50 m, 50 °C, 85 °C for 5 m and lastly for 20 m, 37 °C. For Taqman, 100 ng of RNA input was used and reverse transcription was performed using the setting of: 16 °C, 30 m, 42 °C, 30 m, 85 °C, 5 m, then hold at 4 °C.

For quantitative RT-PCR, the thermal profile for the cDNA obtained in the earlier section was set as follows: 95 °C, 20 s, 95 °C, 1 s followed by 60 °C, 20 s for 40 cycles. The thermal profile for miR-155 and U6 snRNA (endogenous control) was set as follows: 95 °C, 10 m, 95 °C, 15 s followed by 60 °C, 60 s. Cycle threshold (C_T) values were quantified by the use of AB 7900HT Fast Real Time PCR System equipped with sequence detection system software (Sequence Detection System, version 2.1.1; Applied Biosystems) in 96-well plate.

2.6. Luciferase reporter assay

$1.5x10^4$ cells were seeded in 24-well plate containing RPMI supplemented with serum without antibiotics. Cells were transfected using 0.6 μl of FuGENE®6 Transfection Reagent (Roche) with 0.2 μg of the reporter vector. These were achieved by diluting 0.2 μg of the reporter vector in 20 μl of serum-free culture media. pMiR-Luc Reporter Vector for miR-155 (Signosis)/FuGENE®6 complexes were then incubated for 30 m before added into the complete growth medium (to a final volume of 500 μl). The cells were incubated overnight and then exposed to AuNP for another 48 h. Cells were lysed and firefly luciferase reporter activity was measured using the Luciferase Assay System (Promega) according to the manufacturer instructions. The firefly luminescence was measured and data were expressed as mean activities ± S.E from four independent experiments.

2.7. Silencing miR-155 in MRC5 cells

Anti-miR™ miR-155 (Ambion) was used to inhibit the endogenous miR-155 to analyse the effect it has on biological processes. Transfection was done with scrambled miR-control (i.e. negative control) and anti-miR-155 complementary to miRNA utilized in this study. The sequence of the miRNA inhibitor used in our studies can be retrieved from Anti-miR™ miRNA Inhibitors and Libraries (Ambion). The mature miR-155 sequence was UUAAUGCUAAUCGUGAUAGGGGU. Tentatively, the miR-155 sequence can be found from the microRNAs Registry [29] or from the website of Sanger miRBase database [30–32]. Knockdown of miR-155 in MRC5 cells was achieved using HiPerFect Transfection Reagent (Qiagen). Transfection reactions were run in triplicate. Transfection efficiency was pre-optimized in MRC5 cells by adjusting parameters such as cell density, length of exposure, amount of transfect reagent and anti-miR-155 oligonucleotide. Transfection complexes were prepared according to the user guide of the reagent manufacturer and added to the cells at a final anti-mir-155 concentration of 20 nM. Fresh RPMI complete culture medium was used to replace the old medium post 24 h after transfection. The cells were incubated for another 24 h. Following 48 h of incubation, RNA or protein was extracted for subsequent assays. Experiments were conducted in triplicates.

2.8. Western blot analysis

Briefly, protein was extracted using MPER (Pierce Biotechnology) added with EDTA, phosphatase inhibitor and protease inhibitor (Pierce Biotechnology) which prevents the protein of interest from degradation. The amount of protein was quantified using Protein Assay kit (Bio-Rad). The protein sample was separated using 10% sodium dodecyl sulfate–polyacrylamide gel by electrophoresis (SDS-PAGE) before transferred to a PVDF membrane (Bio-Rad) for detection. The membrane was incubated with 5% milk for 1 h. PROS1 (Abcam) or beta-actin (as internal loading control) (Bio-Rad) antibody was then added to allow binding to their respective specific proteins. Following an overnight incubation at 4 °C, secondary antibody-HRP conjugate (Amersham Biosciences) was added. The targeted protein bands were visualized at 75 (PROS1) and 42 kDa (beta-actin) using SuperSignal West Pico Chemiluminescent Substrate (Pierce Biotechnology). Bands were quantified by densitometer GS-710 (Bio-Rad).

2.9. Bisulfite sequencing of methylated PROS1

Total genomic DNA was extracted using DNeasy Blood and Tissue Kit (Qiagen) according to the manufacturer protocol, which included the Proteinase K digestion step. Bisulfite conversion of genomic DNA was performed using EpiTect Bisulfite Kit (Qiagen) for conversion of unmethylated cytosines nucleotides to discriminate from methylated cytosines (U (T) –nucleotides). Briefly, 1 μg of DNA was subjected to sodium bisulfite treatment, denatured at 95 °C for 5 m, and bisulfite converted at 60 °C. DNA samples were then desulphonated, cleaned and eluted.

Next, bisulfite-conversion-based methylation PCR primers were first designed to amplify bisulfite converted methylated and unmethylated DNA but not unmodified DNA using Methyl Primer Express® Software (Applied Biosystems). Bisulfite Sequencing PCR (BSP) was used for PROS1 DNA methylation quantification through sequencing later. The sequences of BSP primer used in this study were: Forward: 5′ ATATGTGGATGATTAAAATGAT 3′; Reverse: 5′AACACTACTAAAACATCCTTCT 3′. Amplification of PROS1 was performed using GoTaq® Colorless Master Mix (Promega).

Subcloning of methylated PROS1 cDNA was performed using an expression pDrive Cloning Vector (Qiagen). Purified cloning product was subjected to verification of the correct sized insert via PCR before sequencing (1st BASE). For analysis purpose, sequences were aligned using BiQ Analyzer [33] (Max-Planck) to generate lollipop grid to determine the degree of methylation.

2.10. TissueScan™ qPCR Array

TissueScan Human Normal (48 Tissues) qPCR array which comprises a panel of pre-normalized cDNA (OriGene) was analyzed by real-time PCR using the Applied Biosystems 7500 Real-Time PCR System. The specific PROS1 primers used were forward 5′- CCTAGTGCTTCCCGTCTCAG-3′; reverse 5′-TTTCCGGGTCATTTTCAAAG-3′.

2.11. Statistical analysis

The Student's *t*-test was used to analyse differences between two groups and One Way ANOVA with post hoc test (Tukey's Multiple Comparison Test) for comparing three or more groups of data. Data are reported as mean values ±SEM. *P* values of less than 0.05 were considered statistically significant, and all statistical calculations were carried out using Graph Pad Prism Version 5.0 (GraphPad Software).

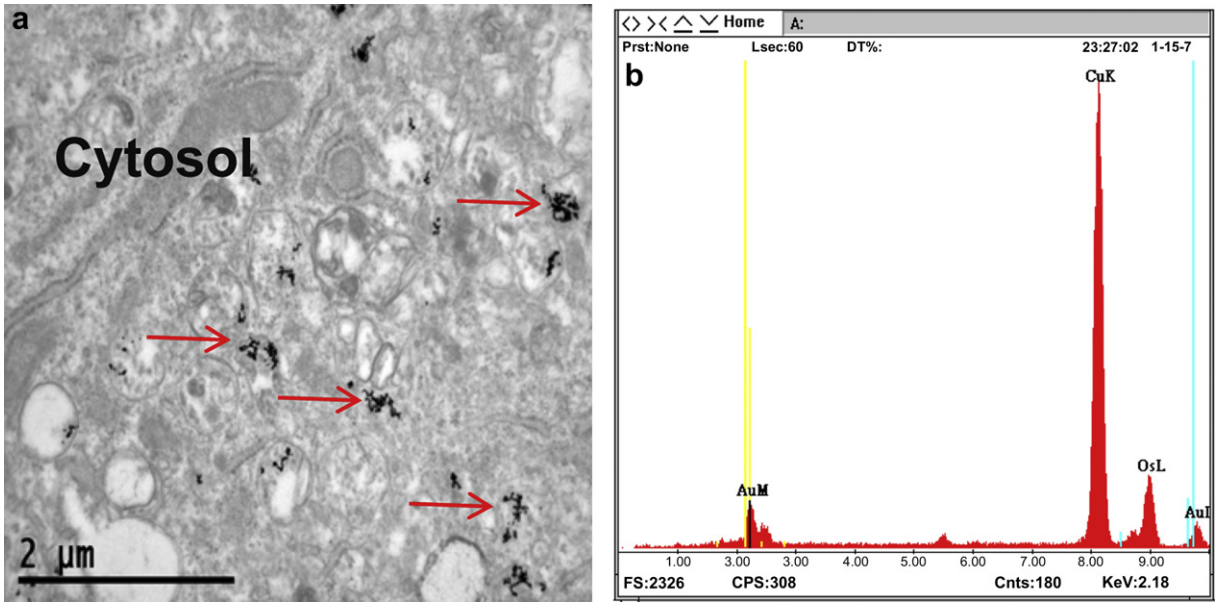

Fig. 1. Ultrastructural localization of AuNPs. (a) AuNPs were taken up by MRC5 cells (red arrows) and localized predominantly as clusters in the cytoplasm, with some AuNPs enclosed within the endosomes. Magnification: 14000× (b) EDAX elemental analysis confirmed the presence of Au as depicted by two sharp peaks at 2.121 keV (AuL) and 9.712 keV (AuM). (For interpretation of the references to colour in this figure legend, the reader is referred to the web version of this article.)

3. Results and Discussions

3.1. Intracellular localization of AuNPs in MRC5 lung fibroblasts

The cellular uptake of AuNP by MRC5 was confirmed by TEM. After 72 h of 1 nM AuNP treatment (concentration obtained from our previous studies [25,26]), the AuNPs were found to be localized mainly as clusters in the cytoplasm of the lung fibroblasts (Fig. 1a). Using EDAX Microanalysis, electron dense deposits were verified to be Au (Fig. 1b).

Table 1
Modulation of genes detected by Affymetrix Gene Analysis in AuNP-treated MRC5 lung fibroblasts. All genes have at least a 1.5 fold change in AuNP-treated MRC5 lung fibroblasts compared to control, with $p < 0.05$.

Gene name (description)	Gene Accession	Fold change
Up-regulated genes		
FLJ10246	AK001108	1.70
SLC38A5	NM_033518	1.69
ZC3HAV1	NM_080660	1.60
VEGFC	NM_005429	1.60
ITGA2	NM_002203	1.59
RELN	NM_005045	1.58
MIRNA155	NR_001458	1.56
ATP10A	NM_024490	1.53
ADAR	NM_001033049	1.52
Down-regulated genes		
SC4MOL	NM_006745	1.91
TAF9B|LOC728198	NM_015975	1.88
PROS1	M15036	1.85
C5orf21	NM_018356	1.82
FAP	NM_004460	1.75
IDI1	NM_004508	1.66
ZMAT3	NM_022470	1.60
TRPA1	NM_007332	1.59
STYX|LOC730432	NM_145251	1.51
RFTN2	NM_144629	1.51

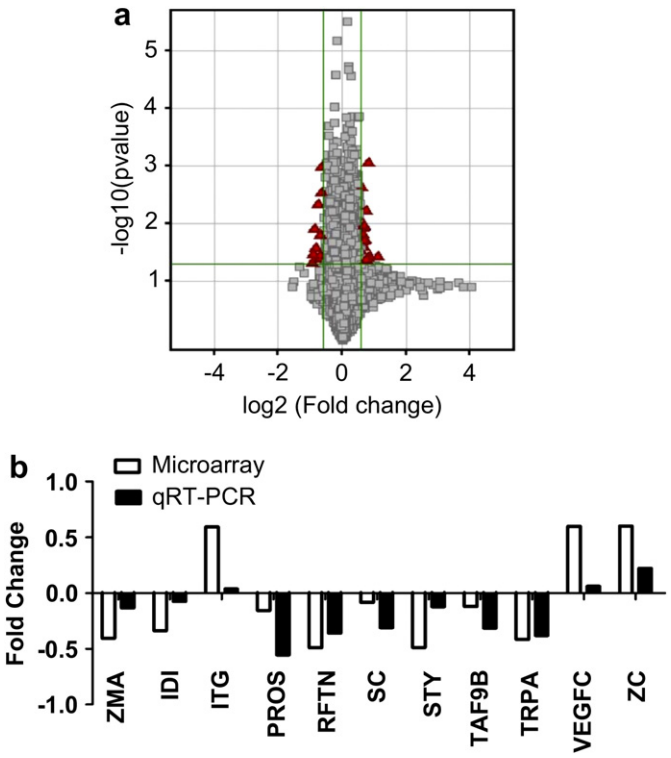

Fig. 2. Global gene micro-array in lung fibroblasts after treatment with AuNPs. (a) Volcano plot to compare the transcriptomes of MRC5 cells treated with AuNP against cells not exposed to the nanoparticles. The analysis was carried out using GeneSpring GX v11.5. The list of candidate genes was generated using the filtering criteria of $p < 0.05$ and fold change of at least 1.5 after Robust Multiarray Average (RMA) normalisation. The red triangles represent genes that fulfilled these criteria, while genes that did not satisfy these conditions are shown as grey squares. (b) Selected gene expression profiles derived from micro-array were verified by q(RT)-PCR which showed concordance. (For interpretation of the references to colour in this figure legend, the reader is referred to the web version of this article.)

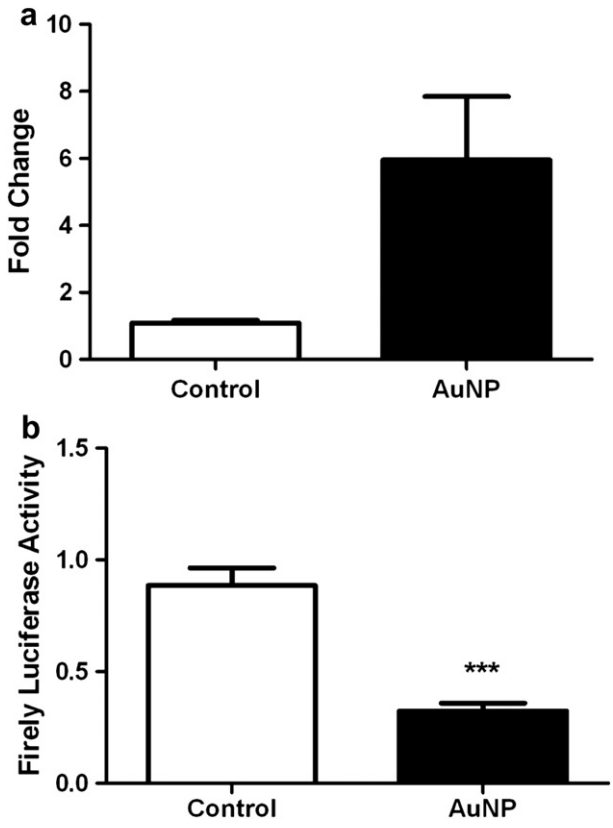

Fig. 3. Validation of miR-155 expression after AuNP exposure. (a) Bar chart of miR-155 gene expression in MRC5 lung fibroblasts using u6 snRNA as a normalizer. (b) Samples in 24-well plate consisted of MRC5 cells ($\sim 1.5 \times 10^4$ per well) that were stably transfected with the pMiR-Luc Reporter Vector for miR-155 followed by 48 h post AuNP exposure. Firely luciferase activities of AuNP-treated fibroblasts and controls were measured in a 24-well plate reader for luminometry. Error bar = Standard error of the mean. ***$p < 0.001$ compared with untreated cells.

3.2. Differential regulation of genes in lung fibroblasts treated with AuNPs

The global gene expression profile of control and AuNP-treated human lung fibroblasts was compared using the Affymetrix Human Gene 1.0 ST Array comprising 28,869 genes. 19 genes were found to be differentially expressed with up-regulation of 9 genes and concomitant down-regulation of 10 genes in AuNP-treated cells (Table 1 and Fig. 2a). 11 genes were selected for verification through real-time RT-PCR and their expression levels were in consistent with the data derived from micro-array analysis (Fig. 2b). Meanwhile, the differentially expressed genes can be classified into stress-responsive genes and genes that regulate cellular morphogenesis, blood coagulation, hemostasis, hydrolase activity, metal ion binding and sterol metabolism [34,35], as shown in Supplementary Table 1. Genes related to sterol biosynthetic process, such as isopentenyl-diphosphate delta isomerase 1 (IDI1) and sterol-C4-methyl oxidase-like (SC4MOL) are associated with synthesis of cholesterol [36–38] while other identified genes participate in various cellular pathways, where dysregulation may cause pathogenesis of diseases.

3.3. Modulation of miR-155 induced by AuNP exposure

A gene of interest from the micro-array analysis is up-regulation of the non-protein coding RNA, microRNA 155 (miR-155, Table 1) concomitant with down-regulation of 10 other genes (including the

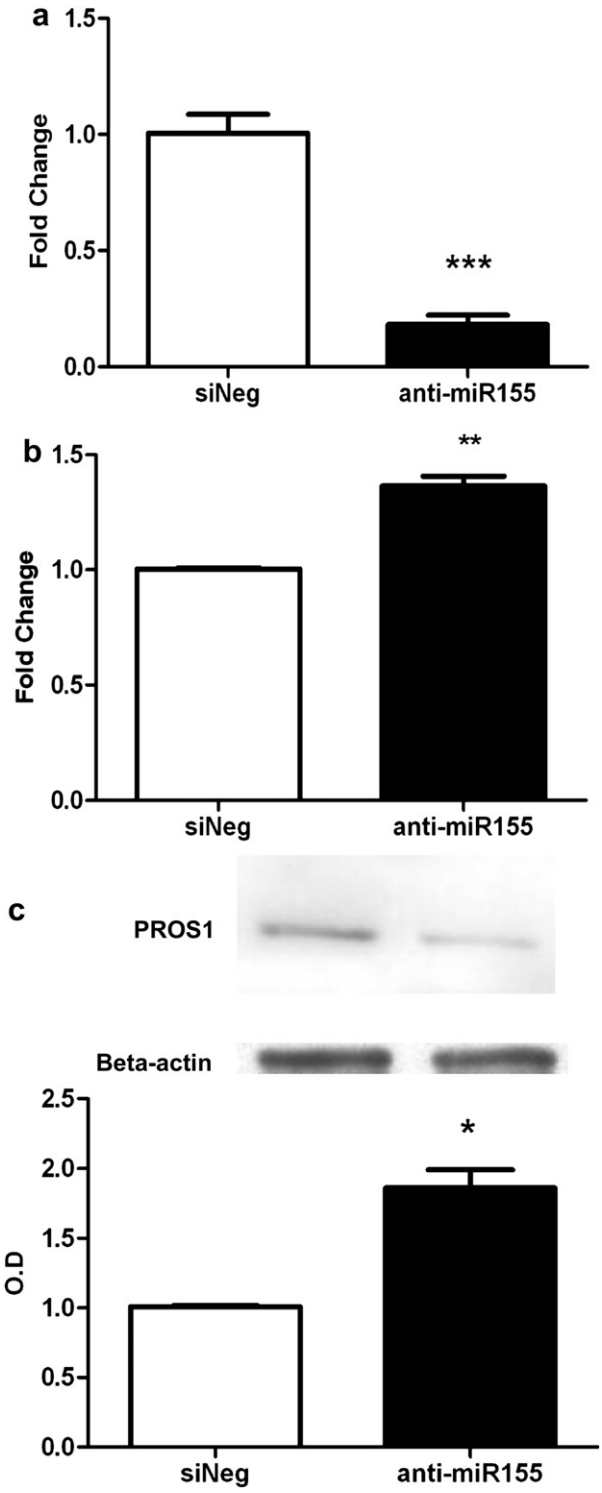

Fig. 4. miR-155 modulates PROS1 expression in lung fibroblasts. (a) miR-155 silencing efficiency. Error bar = Standard error of the mean. ***$p < 0.001$ compared with negative control cells. (b) Silencing of miR-155 gene induced an up-regulation of PROS1 protein expression. MRC5 fibroblasts were treated with anti-miR-155 and anti-miR™ miRNA inhibitors negative control. Error bar = Standard error of the mean. **$p < 0.01$ (c) Protein bands from Western blot analysis with antibodies against PROS1 and beta-actin (housekeeping protein). Bar chart shows the optical densities of the PROS1 protein bands normalized against beta-actin. Error bar = Standard error of the mean. *$p < 0.05$ compared with negative control cells.

PROS1 gene) in AuNP treated fibroblasts. miR-155 up-regulation after AuNP exposure was verified by RT-PCR analysis using the Taqman probe and u6 snRNA as endogenous reference genes (Fig. 3a). However, no significant difference was observed between control and AuNP-treated groups. We further attempted to validate miR-155 induction by using reporter assay containing a firefly luciferase construct contains a target site that is complementary to miR-155. We observed that AuNPs repressed firefly luciferase activity by 63% in MRC5 fibroblasts transfected with the pmiR-155-Luc reporter, showing increased turnover of mRNAs in AuNP-treated cells (Fig. 3b). This is the first report that AuNPs can modulate the expression of miR-155.

Aberrant expression of miRNAs has been implicated in the pathogenesis of diseases [15–19], not surprisingly carcinogenesis [20–22]. In murine breast cancer cells, miR-155 has been shown to directly inhibit expression of *RhoA*, promoting cell migration and invasion [41]. Thus far, miR-155 is known to participate in cellular pathways, such as LPS signaling pathway [39], TGF-β/Smad pathway [40], MAPK signaling pathway [9], angiotensin II-induced extracellular signal-related kinase 1/2 (ERK1/2) activation [41], miR155-mediated pathway of AID regulation [42], regulation of type 1 Angiotensin II receptor (AT1R) [43], PI3K/Akt pathway (which subsequently affects the TNFα-dependent growth of B cell lymphomas) [9,44,45]. These pathways contribute to pathological conditions such as inflammation, carcinogenesis and cardiovascular diseases [43].

3.4. Correlation of PROS1 gene with miR-155

Given that miR-155 performs its biological function by regulating the target protein-coding genes, we analyzed the predicted

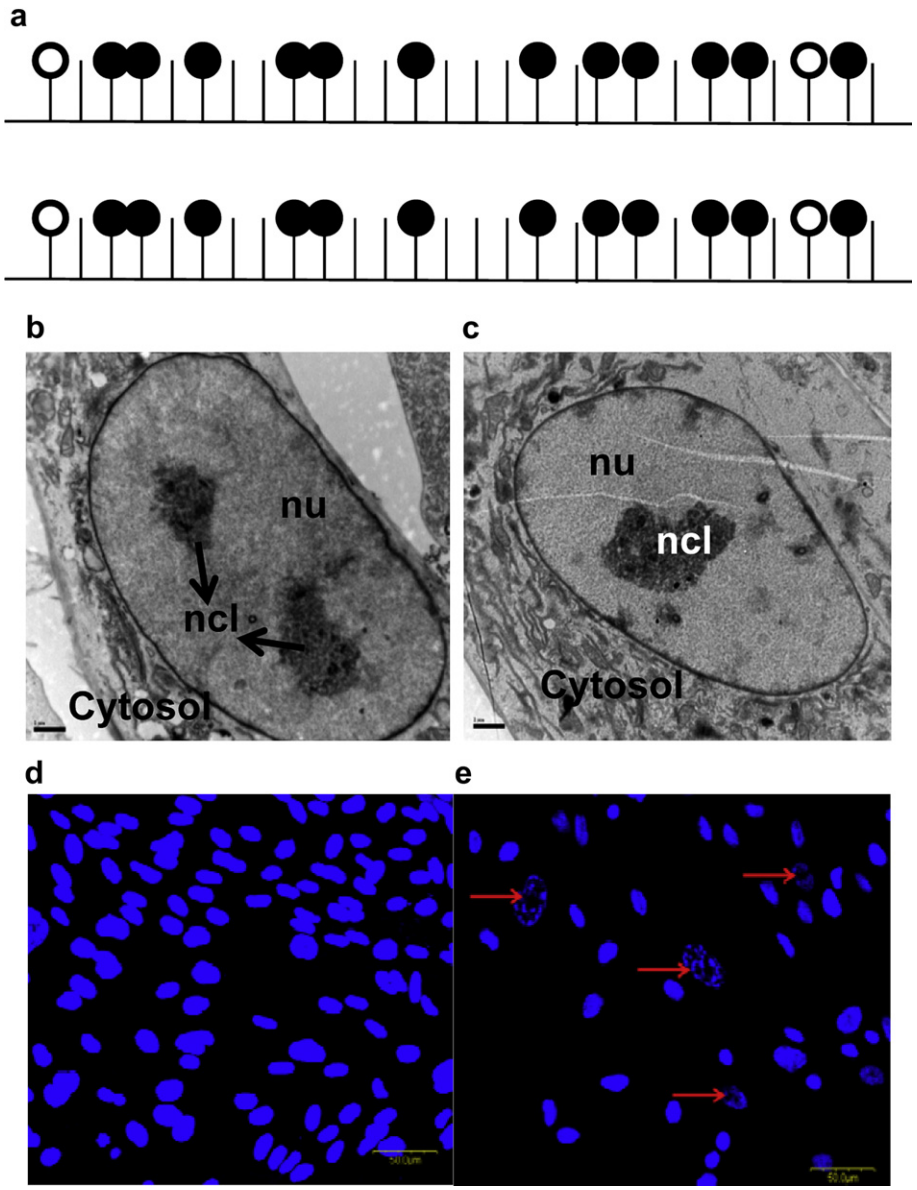

Fig. 5. Epigenetic regulation of PROS1. (a) "Lollipop" schematic diagram of methylation patterns of the PROS1 promoter CpG island region using ClustalW (1.83) multiple sequence alignments. Each "lollipop" summarizes the methylation data after bisulfite sequencing of PROS1 genes. Results from untreated samples and AuNP treated samples are shown. Black lollipops correspond to a methylated C; white lollipops correspond to an unmethylated C; and a stick corresponds to a non-CpG position. (b) Transmission electron micrograph of untreated lung fibroblasts showing the nucleolus (ncl) and euchromatin in the nucleus. Magnification: 5600× (c) Condensation of heterochromatin is seen as clumps in the nucleus of AuNP-treated fibroblast. Magnification: 5600×. (d) Confocal microscopy image of the nuclei of untreated fibroblasts which are stained blue by the DAPI dye. (Scale bar: 50 μm) (e) Chromatin condensation appears as dense areas with increased DAPI staining intensity in the nuclei of AuNP-treated fibroblasts. (Scale bar: 50 μm). (For interpretation of the references to colour in this figure legend, the reader is referred to the web version of this article.)

targets of miR-155 using six miRBase algorithms, PicTar (http://pictar.mdc-berlin.de) [46,47], TarBase, miRanda (http://microrna.sanger.ac.uk) and TargetScan Release 5.1 (http://www.targetscan.org), mirBase (http://www.mirbase.org/) and MicroCosm Targets Version 5. However, none of the differentially expressed genes from our micro-array data matched the potential predicted miR-155 targets.

To better understand the biological role of miR-155 in this experimental setting, we performed anti-miR-155 mediated silencing in lung fibroblasts to observe for any altered expression of the other 10 down-regulated genes from the micro-array data. For this purpose, lung fibroblasts were transfected with anti-miR-155. Anti-miR-155 effectively reduced miR-155 expression with a knock down efficiency of 81.8% ($p < 0.001$) (Fig. 4a). We observed that silencing of miR-155 increased the expression of PROS1 at mRNA and protein levels (Fig. 4b and c). Taken together, these results suggest that although endogenous miR-155 is expressed at relatively low level in the lung fibroblasts, inhibition of its expression resulted in enhanced levels of PROS1 expression, indicating that miR-155 could regulate expression of PROS1. However, this change of PROS1 might be indirect, as its 3′UTR does not contain a miR-155 target sequence and therefore is unlikely to be a direct target of miR-155 [48].

A recent paper on mice exposed to surface-coated titanium dioxide NPs by inhalation showed up-regulation of miR-449a, miR-1, and miR-135b with evidence of inflammation in the lung tissues [49]. Our finding that miR-155 inhibits PROS1 expression has clinical significance as Protein S deficiency can lead to thrombosis in the pulmonary vasculature giving rise to adverse outcomes such as lung infraction culminating in death [50] and pulmonary hypertension [51]. The PROS1 gene encodes for Protein S, a vitamin K–dependent plasma glycoprotein that participates in the inactivation of Factors Va and VIIIa which are involved in thrombus formation [52]. Lack of protein S synthesis can lead to coagulopathy such as venous thrombosis giving rise to dire consequences [53]. Protein S has been reported to be synthesized mainly in hepatocytes, megakaryocytes, endothelial cells, and interstitial Leydig cells [54]. To ensure that the PROS1 gene is also expressed in lung tissues, we quantified the levels of PROS1 mRNA in a commercially available normal tissue array covering 48 different human tissues. PROS1 was detected in 45/48 normal tissues, except for lymphocytes, mammary gland and muscle (Fig. S1 in Supplementary Information). The highest expression the PROS1 gene was detected in lung tissue, followed by small intestine, adrenal gland, uterus, pituitary, heart, stomach, penis, ovary and liver.

3.5. Sequencing-based PROS1 DNA methylation profiling analysis and chromatin reorganization/heterochromatin formation in MRC5 induced by AuNPs

It was reported that dysregulation of miRNAs is known to cause other epigenetic changes such as aberrant DNA methylation [55–57]. However, we found that the DNA methylation profile of the PROS1 gene was unaffected by AuNP treatment as analyzed by bisulfite sequencing (Fig. 5a), indicating that there was no AuNP-induced epigenetic modifications on the DNA methylation status. Since miRNAs are also known to act as negative gene regulators via chromatin remodeling [58,59], we evaluated nuclear changes induced by AuNP treatment in the lung fibroblasts. Transmission electron microscopy (TEM) revealed the presence of chromatin condensation in AuNP-treated fibroblasts in comparison with untreated fibroblasts (Fig. 5b and c). There was also apparent reorganization of nuclear content and chromatin condensation in AuNP-treated lung fibroblasts observed under confocal microscope (Fig. 5e), complementing the TEM results.

4. Conclusion

We investigated the effects of AuNP exposure on the genomic profile of lung fibroblasts *in vitro*. We detected up-regulation of miR-155 in AuNP-treated lung fibroblasts and ascertained that PROS1 gene is a putative target gene of miR-155. We observed that cells undergo nuclear chromatin condensation in response to AuNP exposure. However, more studies are needed as little is currently known about whether miR-155 interacts with chromatin regulatory components and chromatin-binding/-modifying proteins in the formation of a condensed chromatin state and whether miR-155 repress gene transcription by promoting aberrant chromatin modifications. Therefore, future works are needed to address the relationship between the epigenomic landscape and disease states induced by NPs. Consistency in monitoring the effects of human health and environment and special guidelines and precaution are required to minimize their toxicological effects.

Acknowledgements

The author would like to thank Mr. Deny Hartono for synthesizing AuNP used in this study. This work was supported by research funding from the Singapore Ministry of Education Academic Research Fund Tier 2 via grant MOE2008-T2-1-046.

Appendix. Supplementary material

Supplementary data associated with this article can be found, in the online version, at doi:10.1016/j.biomaterials.2011.06.038.

References

[1] Warheit DB, Sayes CM, Reed KL, Swain KA. Health effects related to nanoparticle exposures: environmental, health and safety considerations for assessing hazards and risks. Pharmacol Ther 2008;120(1):35–42.
[2] Nowack B, Bucheli TD. Occurrence, behavior and effects of nanoparticles in the environment. Environ Pollut 2007;150(1):5–22.
[3] Murphy CJ, Gole AM, Stone JW, Sisco PN, Alkilany AM, Goldsmith EC, et al. Gold nanoparticles in biology: beyond toxicity to cellular imaging. Acc Chem Res 2008;41(12):1721–30.
[4] Leduc C, Jung JM, Carney RR, Stellacci F, Lounis B. Direct investigation of intracellular presence of gold nanoparticles via photothermal heterodyne imaging. ACS Nano 2011;5(4):2587–92.
[5] Lewinski N, Colvin V, Drezek R. Cytotoxicity of nanoparticles. Small 2008;4(1):26–49.
[6] Singh N, Manshian B, Jenkins GJ, Griffiths SM, Williams PM, Maffeis TG, et al. NanoGenotoxicology: the DNA damaging potential of engineered nanomaterials. Biomaterials 2009;30(23–24):3891–914.
[7] Divekar AA, Dubey S, Gangalum PR, Singh RR. Dicer insufficiency and microRNA-155 overexpression in lupus regulatory T cells: an apparent paradox in the setting of an inflammatory milieu. J Immunol 2011;186(2):924–30.
[8] Kuhn DE, Nuovo GJ, Terry Jr AV, Martin MM, Malana GE, Sansom SE, et al. Chromosome 21-derived microRNAs provide an etiological basis for aberrant protein expression in human Down syndrome brains. J Biol Chem 2010;285(2):1529–43.
[9] Bhattacharyya S, Balakathiresan NS, Dalgard C, Gutti U, Armistead D, Jozwik C, et al. Elevated miR-155 promotes inflammation in cystic fibrosis by driving hyper-expression of interleukin-8. J Biol Chem 2011;286(13):11604–15.
[10] Kuhn DE, Martin MM, Feldman DS, Terry Jr AV, Nuovo GJ, Elton TS. Experimental validation of miRNA targets. Methods 2008;44(1):47–54.
[11] Nakahara K, Kim K, Sciulli C, Dowd SR, Minden JS, Carthew RW. Targets of microRNA regulation in the Drosophila oocyte proteome. Proc Natl Acad Sci U S A 2005;102(34):12023–8.
[12] Esau C, Kang X, Peralta E, Hanson E, Marcusson EG, Ravichandran LV, et al. MicroRNA-143 regulates adipocyte differentiation. J Biol Chem 2004;279(50):52361–5.
[13] Bartel DP. MicroRNAs: genomics, biogenesis, mechanism, and function. Cell 2004;116(2):281–97.
[14] Georgantas 3rd RW, Hildreth R, Morisot S, Alder J, Liu CG, Heimfeld S, et al. CD34+ hematopoietic stem-progenitor cell microRNA expression and function: a circuit diagram of differentiation control. Proc Natl Acad Sci U S A 2007;104(8):2750–5.
[15] Du T, Zamore PD. Beginning to understand microRNA function. Cell Res 2007;17(8):661–3.

[16] Inomata M, Tagawa H, Guo YM, Kameoka Y, Takahashi N, Sawada K. MicroRNA-17-92 down-regulates expression of distinct targets in different B-cell lymphoma subtypes. Blood 2009;113(2):396–402.
[17] Standart N, Jackson RJ. MicroRNAs repress translation of m7Gppp-capped target mRNAs in vitro by inhibiting initiation and promoting deadenylation. Genes Dev 2007;21(16):1975–82.
[18] Pillai RS, Bhattacharyya SN, Filipowicz W. Repression of protein synthesis by miRNAs: how many mechanisms? Trends Cell Biol 2007;17(3):118–26.
[19] Calin GA, Ferracin M, Cimmino A, Di Leva G, Shimizu M, Wojcik SE, et al. A MicroRNA signature associated with prognosis and progression in chronic lymphocytic leukemia. N Engl J Med 2005;353(17):1793–801.
[20] Lee EJ, Gusev Y, Jiang J, Nuovo GJ, Lerner MR, Frankel WL, et al. Expression profiling identifies microRNA signature in pancreatic cancer. Int J Cancer 2007;120(5):1046–54.
[21] Michael MZ, Sm OC, van Holst Pellekaan NG, Young GP, James RJ. Reduced accumulation of specific microRNAs in colorectal neoplasia. Mol Cancer Res 2003;1(12):882–91.
[22] Esquela-Kerscher A, Slack FJ. Oncomirs - microRNAs with a role in cancer. Nat Rev Cancer 2006;6(4):259–69.
[23] Seike M, Goto A, Okano T, Bowman ED, Schetter AJ, Horikawa I, et al. MiR-21 is an EGFR-regulated anti-apoptotic factor in lung cancer in never-smokers. Proc Natl Acad Sci U S A 2009;106(29):12085–90.
[24] Volinia S, Calin GA, Liu CG, Ambs S, Cimmino A, Petrocca F, et al. A microRNA expression signature of human solid tumors defines cancer gene targets. Proc Natl Acad Sci U S A 2006;103(7):2257–61.
[25] Li JJ, Zou L, Hartono D, Ong CN, Bay BH, Yung LYL. Gold nanoparticles induce oxidative damage in lung fibroblasts in vitro. Adv Mater 2008;20(1):138–42.
[26] Li JJ, Hartono D, Ong CN, Bay BH, Yung LYL. Autophagy and oxidative stress associated with gold nanoparticles. Biomaterials 2010;31(23):5996–6003.
[27] Carayol N, Campbell A, Vachier I, Mainprice B, Bousquet J, Godard P, et al. Modulation of cadherin and catenins expression by tumor necrosis factor-alpha and dexamethasone in human bronchial epithelial cells. Am J Respir Cell Mol Biol 2002;26(3):341–7.
[28] Gras D, Tiers L, Vachier I, de Senneville LD, Bourdin A, Godard P, et al. Regulation of CXCR/IL-8 in human airway epithelial cells. Int Arch Allergy Immunol 2010;152(2):140–50.
[29] Griffiths-Jones S. The microRNA Registry. Nucleic Acids Res 2004;32: D109–11.
[30] Griffiths-Jones S, Saini HK, van Dongen S, Enright AJ. miRBase: tools for microRNA genomics. Nucleic Acids Res 2008;36(Database issue):D154–8.
[31] Griffiths-Jones S, Grocock RJ, van Dongen S, Bateman A, Enright AJ. miRBase: microRNA sequences, targets and gene nomenclature. Nucleic Acids Res 2006; 34:D140–4.
[32] Ambros V, Bartel B, Bartel DP, Burge CB, Carrington JC, Chen X, et al. A uniform system for microRNA annotation. RNA 2003;9(3):277–9.
[33] Bock C, Reither S, Mikeska T, Paulsen M, Walter J, Lengauer T. BiQ Analyzer: visualization and quality control for DNA methylation data from bisulfite sequencing. Bioinformatics 2005;21(21):4067–8.
[34] Huang da W, Sherman BT, Lempicki RA. Systematic and integrative analysis of large gene lists using DAVID bioinformatics resources. Nat Protoc 2009;4(1):44–57.
[35 Dennis Jr G, Sherman BT, Hosack DA, Yang J, Gao W, Lane HC, et al. DAVID: database for annotation, visualization, and Integrated Discovery. Genome Biol 2003;4(5):P3.
[36] Steiner S, Gatlin CL, Lennon JJ, McGrath AM, Seonarain MD, Makusky AJ, et al. Cholesterol biosynthesis regulation and protein changes in rat liver following treatment with fluvastatin. Toxicol Lett 2001;120(1–3):369–77.
[37] Sato Y, Koshioka S, Kirino Y, Kamimoto T, Kawazoe K, Abe S, et al. Role of dipeptidyl peptidase IV (DPP4) in the development of dyslipidemia: DPP4 contributes to the steroid metabolism pathway. Life Sci 2011;88(1–2):43–9.
[38] Oger E, Ghignone S, Campagnac E, Fontaine J, Grandmougin-Ferjani A, Lanfranco L. Functional characterization of a C-4 sterol methyl oxidase from the endomycorrhizal fungus Glomus intraradices. Fungal Genet Biol 2009; 46(6–7):486–95.
[39] Boesch-Saadatmandi C, Loboda A, Wagner AE, Stachurska A, Jozkowicz A, Dulak J, et al. Effect of quercetin and its metabolites isorhamnetin and quercetin-3-glucuronide on inflammatory gene expression: role of miR-155. J Nutr Biochem 2010;22(3):293–9.
[40] Kong W, Yang H, He L, Zhao JJ, Coppola D, Dalton WS, et al. MicroRNA-155 is regulated by the transforming growth factor beta/Smad pathway and contributes to epithelial cell plasticity by targeting RhoA. Mol Cell Biol 2008; 28(22):6773–84.
[41] Martin MM, Lee EJ, Buckenberger JA, Schmittgen TD, Elton TS. MicroRNA-155 regulates human angiotensin II type 1 receptor expression in fibroblasts. J Biol Chem 2006;281(27):18277–84.
[42] Teng G, Hakimpour P, Landgraf P, Rice A, Tuschl T, Casellas R, et al. MicroRNA-155 is a negative regulator of activation-induced cytidine deaminase. Immunity 2008;28(5):621–9.
[43] Faraoni I, Antonetti FR, Cardone J, Bonmassar E. miR-155 gene: a typical multifunctional microRNA. Biochim Biophys Acta 2009;1792(6):497–505.
[44] Cremer TJ, Ravneberg DH, Clay CD, Piper-Hunter MG, Marsh CB, Elton TS, et al. MiR-155 induction by F. novicida but not the virulent F. tularensis results in SHIP down-regulation and enhanced pro-inflammatory cytokine response. PLoS One 2009;4(12):e8508.
[45] Pedersen IM, Otero D, Kao E, Miletic AV, Hother C, Ralfkiaer E, et al. Onco-miR-155 targets SHIP1 to promote TNFalpha-dependent growth of B cell lymphomas. EMBO Mol Med 2009;1(5):288–95.
[46] Krek A, Grun D, Poy MN, Wolf R, Rosenberg L, Epstein EJ, et al. Combinatorial microRNA target predictions. Nat Genet 2005;37(5):495–500.
[47] Grun D, Wang YL, Langenberger D, Gunsalus KC, Rajewsky N. microRNA target predictions across seven Drosophila species and comparison to mammalian targets. PLoS Comput Biol 2005;1(1):e13.
[48] Yang X, Feng M, Jiang X, Wu Z, Li Z, Aau M, et al. miR-449a and miR-449b are direct transcriptional targets of E2F1 and negatively regulate pRb-E2F1 activity through a feedback loop by targeting CDK6 and CDC25A. Genes Dev 2009;23(20):2388–93.
[49] Halappanavar S, Jackson P, Williams A, Jensen KA, Hougaard KS, Vogel U, et al. Pulmonary response to surface-coated nanotitanium dioxide particles includes induction of acute phase response genes, inflammatory cascades, and changes in microRNAs: a toxicogenomic study. Environ Mol Mutagen; 2011. Epub ahead of print.
[50] Zander DS, Baz MA, Visner GA, Staples ED, Donnelly WH, Faro A, et al. Analysis of early deaths after isolated lung transplantation. Chest 2001;120(1):225–32.
[51] Piazza G, Goldhaber SZ. Chronic thromboembolic pulmonary hypertension. N Engl J Med 2011;364(4):351–60.
[52] Simioni P, Tormene D, Spiezia L, Tognin G, Rossetto V, Radu C, et al. Inherited thrombophilia and venous thromboembolism. Semin Thromb Hemost 2006; 32(7):700–8.
[53] Lijfering WM, Mulder R, ten Kate MK, Veeger NJ, Mulder AB, van der Meer J. Clinical relevance of decreased free protein S levels: results from a retrospective family cohort study involving 1143 relatives. Blood 2009;113(6): 1225–30.
[54] ten Kate MK, van der Meer J. Protein S deficiency: a clinical perspective. Haemophilia 2008;14(6):1222–8.
[55] Gao W, Yu Y, Cao H, Shen H, Li X, Pan S, et al. Deregulated expression of miR-21, miR-143 and miR-181a in non small cell lung cancer is related to clinicopathologic characteristics or patient prognosis. Biomed Pharmacother 2010;64(6):399–408.
[56] Calin GA, Croce CM. . MicroRNA signatures in human cancers. Nat Rev Cancer 2006;6:857–66.
[57] Kuhn DE, Nuovo GJ, Martin MM, Malana GE, Pleister AP, Jiang J, et al. Human chromosome 21-derived miRNAs are overexpressed in down syndrome brains and hearts. Biochem Biophys Res Commun 2008;370(3):473–7.
[58] Finnegan EJ, Matzke MA. The small RNA world. J Cell Sci 2003;116(23): 4689–93.
[59] Gonzalez S, Pisano DG, Serrano M. Mechanistic principles of chromatin remodeling guided by siRNAs and miRNAs. Cell Cycle 2008;7(16):2601–8.